Applied Surface Science 255 (2008) 2333–2337

Contents lists available at ScienceDirect

Applied Surface Science

journal homepage: www.elsevier.com/locate/apsusc

Surface topography and morphology characterization of PIII irradiated silicon surface

Satinder K. Sharma, Sumit Barthwal *

Nano Science and Nanotechnology Unit, Department of Chemical Engineering, Indian Institute of Technology (IIT), Kanpur 208016, India

ARTICLE INFO

Article history:
Received 5 January 2008
Received in revised form 19 June 2008
Accepted 16 July 2008
Available online 5 August 2008

Keywords:
PIII
Surface modification
Silicon islands
AFM and micro-Raman

ABSTRACT

The effect of plasma immersion ion implantation (PIII) treatment on silicon surfaces was investigated by micro-Raman and atomic force microscopy (AFM) technique. The surface damage was given by the implantation of carbon, nitrogen, oxygen and argon ions using an inductively coupled plasma (ICP) source at low pressure. AFM studies show that surface topography of the PIII treated silicon wafers depend on the physical and chemical nature of the implanted species. Micro-Raman spectra indicate that the significant reduction of intensity of Raman peak after PIII treatment. Plasma immersion ion implantation is a non-line-of-sight ion implantation method, which allows 3D treatment of materials. Therefore, PIII based surface modification and plasma immersion ion deposition (PIID) coatings are applied in a wide range of situations.

1. Introduction

Plasma immersion ion implantation (PIII or PI^3) is a novel ion implantation technique developed recently for the improvement of the surface properties of materials including semiconductors, metals and dielectrics [1,2]. PIII and plasma immersion ion implantation and deposition (PIIID) were originally developed as a revolutionary non-line-of-sight process by incorporating a three dimensionally shaped target (substrate) in the ion acceleration scheme itself, rather than utilizing conventional ion extraction. The object to-be-treated was immersed in the plasma and by being biased, it became part of an ion source in a more general sense. Ion acceleration occurs in a dynamic, self-adjusting sheath that forms around the biased target surface. PIII and PIIID are known by a variety of names, acronyms and trademarks, including, but not limited to the following: plasma source ion implantation (PSII), plasma immersion ion implantation, plasma ion implantation (PII or PI^2), plasma ion plating (PIP), plasma immersion ion implantation and deposition, metal plasma immersion ion implantation and deposition (MePIIID), plasma doping (PLAD), plasma ion immersion processing (PIIP). Some of these names are synonymous; others emphasize a certain aspect such as the presence of metal ions [3–6]. In this work, silicon wafers were implanted with carbon, nitrogen, oxygen and argon ions using PIII technique. The surface topography and morphology studies were carried out by atomic force microscopy and micro-Raman technique.

2. Plasma immersion ion implantation system

Fig. 1 shows a typical diagram of the PIII system used in this work. The plasma is produced by an ICP glow discharge source located inside a vacuum chamber ($<10^{-3}$ mbar). The 3D ion implantation is achieved by applying repetitively a negative high voltage pulse (10–20 kV, 8–12 μs duration times, 5–20 Hz repetition frequencies) to the sheath formed between the plasma and the substrate. While the voltage pulse is present, the sheath boundary propagates outward and before it reaches the chamber walls the high voltage is turned off, terminating the implantation process during that pulse [5]. The presence of grounded conducting grid between source and sample holder, divide this system into two parts as shown in Fig. 1. This grid is made of a compatible material to avoid contamination and decreases the propagation of the plasma sheath. Ions are formed in the plasma sustained by external plasma source above the grid and accelerated through the lower zone to be implanted into sample. It has many advantages over conventional PIII system such as reduction in the expensive of high voltage modulator supply by substituting a DC power supply, metallic contamination due to fewer ions hitting the exposed samples, lowering working gas pressure due to increasing the plasma density and increasing the ion impact energy due to enabling high voltage insulation of the sample holder. This system delivers plasmas with medium electron densities ($n_e > 10^{10}$ cm^{-3})

* Corresponding author. Tel.: +91 512 2597138.
E-mail address: sumitb3@yahoo.co.in (S. Barthwal).

0169-4332/$ – see front matter © 2008 Elsevier B.V. All rights reserved.
doi:10.1016/j.apsusc.2008.07.129

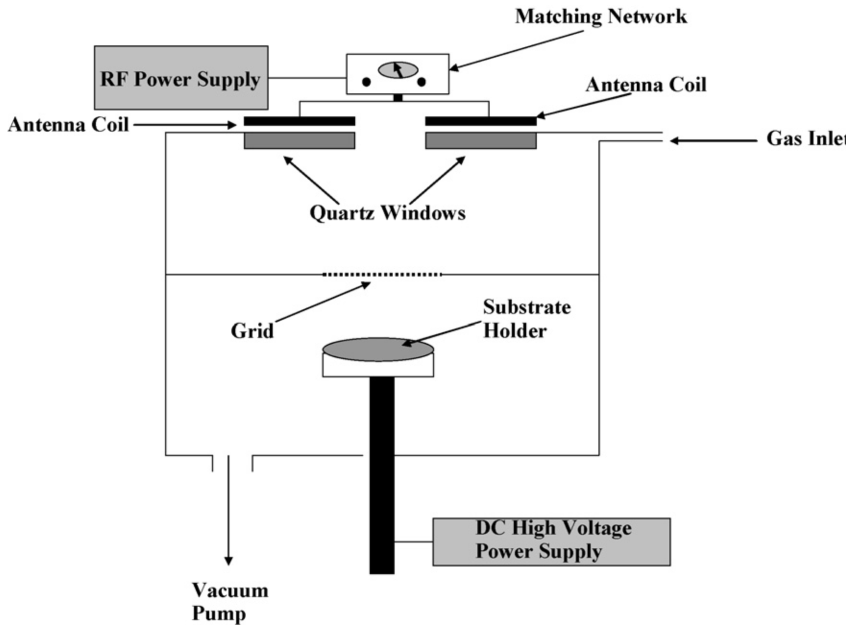

Fig. 1. Schematic representation of plasma immersion ion implantation system.

low electron temperatures ($T_e < 10$ eV), controlled plasma potentials (¢_p) between 0 and 350 V, and with high stability for long operation times (>50 h). These characteristics allied with the possibility of low-pressure operation ($<10^{-3}$ mbar) are highly favourable for the PIII processing of materials.

3. Experimental

P-type ⟨1 0 0⟩ Si wafers of 0.5-mm thick, 4 cm × 4 cm pieces of polished in one side and cleaned by standard Radio Corporation of America (RCA) techniques just before their insertion into the vacuum chamber. They were fixed and masked adequately in a metallic sample holder. These silicon wafers were implanted with carbon, nitrogen, oxygen and argon ions of the plasma potential controlled at $\text{¢}_p = 75$ V, with plasma density of 1×10^{10} cm^{-2}. The high voltage pulser was operated with peak voltage of 50 keV for all experiments, 8 μs pulse duration and repetition frequency of 50 Hz. Based on the sheath propagation model, an implanting dose of 1×10^{15} cm^{-2} is used for 2000 min for all these experiments. After implantation these samples were annealed at 300 °C for 30 min to annihilation of implantation damages. After implantation the surface topography of these samples were characterized by the AFM of Molecular Imaging Company, USA (Pico-Scan). The silicon nitrite tip is used for AFM imaging of scan area 1 μm × 1 μm. Three imaging modes, contact mode, non-contact mode, and intermittent contact or tapping mode, can be used to produce topographic images of sample. In this work non-contact (AAC-AFM) mode is used for topography analysis of the samples.

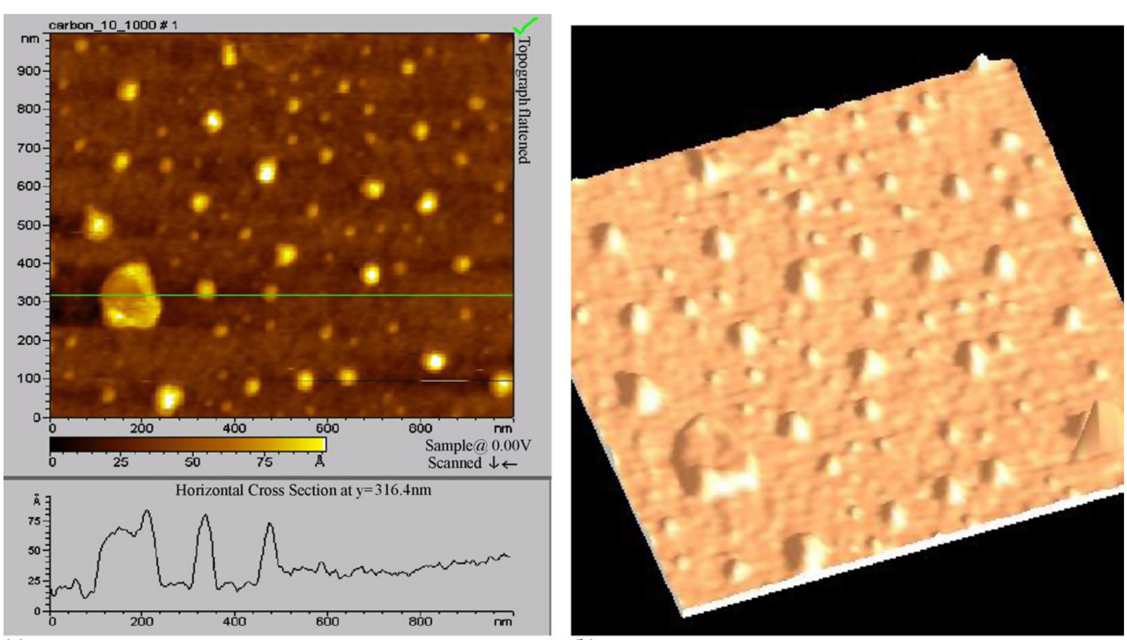

(a) (b)

Fig. 2. 2D (a) and 3D (b) AFM images of carbon PIII treated silicon surface.

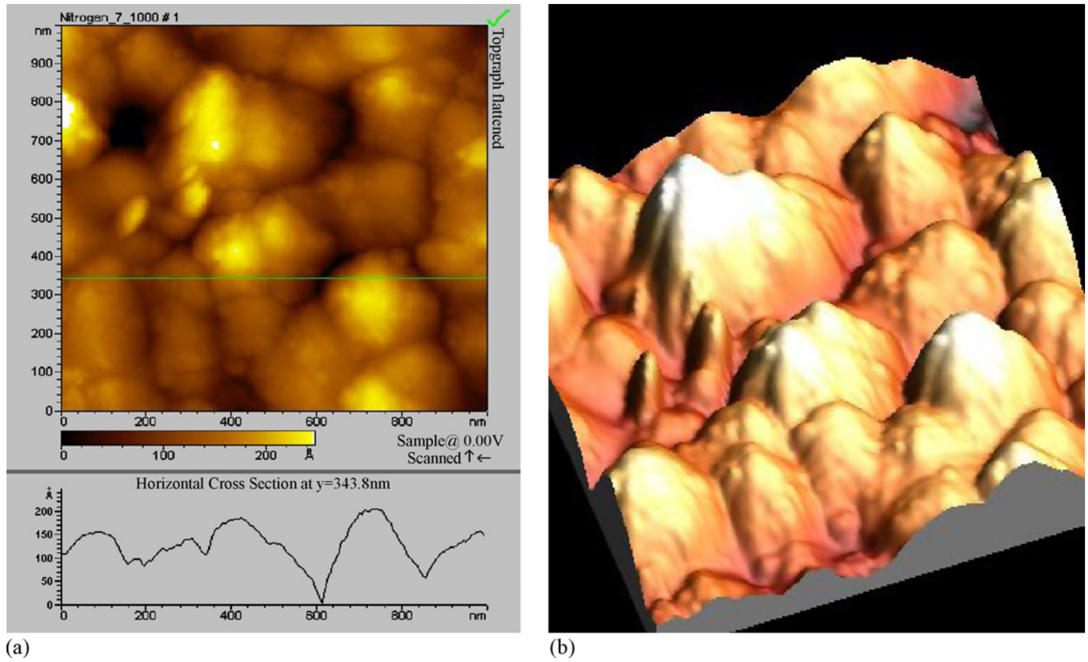

Fig. 3. 2D (a) and 3D (b) AFM images of nitrogen PIII treated silicon surface.

The resonant frequency of silicon cantilever NSC36A of (Mikro-Masch Company) used for analysis of these samples was 125 kHz and force constant 1 N/m.

The disorderness and amorphoziation of implanted silicon wafers were carried out by the WiTec CRM 2000 Raman spectrometer coupled with a high resolution Confocal optical microscope. With this combination it is not only possible to obtain a Raman spectrum of a sample but also to combine its chemical information with a lateral resolution in the sub-micrometer regime. Both the excitation and collection of the scattered light were done through the microscope objective. Excitation was provided by the 532 nm line of an argon ionized laser. The microscope objective used was Nikon 100X, with working distance 0.26. Thus, the laser beam diameter at the focus is approximately in submicron regime. All the measurements were made at room temperature, in order to avoid heating effects in the spectra. Therefore, the measurements were performed at a laser power density below threshold to induce temperature enhancement. All the measured spectra were systematically compared to those obtained on bulk silicon under the same experimental conditions.

4. Results and discussions

AFM and Raman study has actually revealed the dynamic behaviour of surface defects originated from ion clusters after PIII irradiated surfaces. The surface micro-topography changes upon

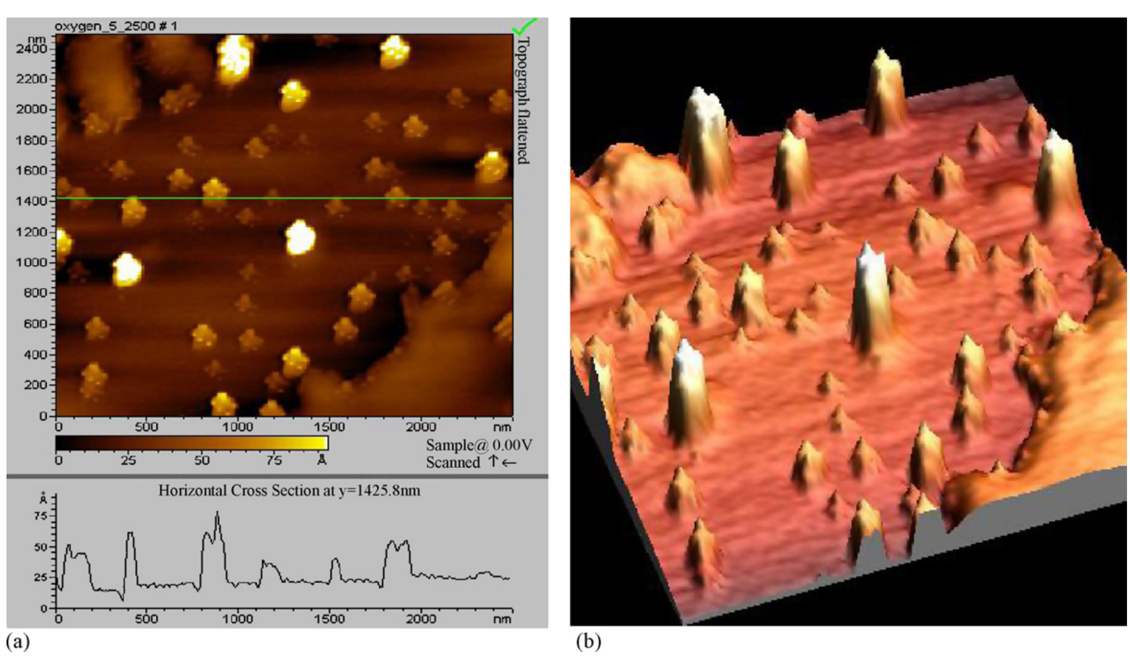

Fig. 4. 2D (a) and 3D (b) AFM images of oxygen PIII treated silicon surface.

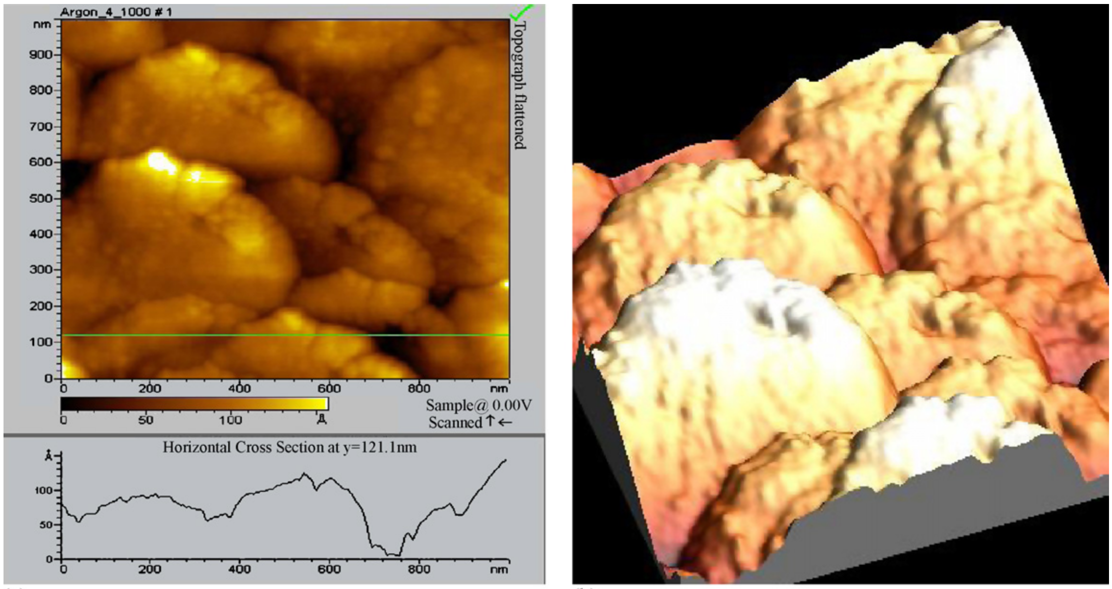

(a) (b)

Fig. 5. 2D and 3D AFM images of argon PIII treated silicon surface.

plasma immersion ion implantation treatment were analyzed by means of AFM technique. Fig. 2 shows the 2D and 3D images of carbon implanted silicon wafers resulted after the implanting dose and energy of 1×10^{15} ions/cm^2 and 50 keV, respectively. The surface topography of nitrogen, oxygen and argon ions implanted silicon wafers at the similar dose and energy have been shown in Figs. 3–5. The PIII irradiated silicon wafers with these implanting species result the occupation of these ions at the interstitials sites in the silicon lattice, this type of non-substitutional behaviour is not surprising [7–9]. It may be expected on the basis of atomic size or covalent radius. The atomic radius of implanted carbon, nitrogen, oxygen and argon ions was 0.91, 0.75, 0.57 and 0.88 Å respectively, while the atomic radius of silicon was 1.17 Å. Therefore, these implanted species with in silicon act as the interstitial impurity rather than sub-substitution impurities, due to the larger difference in the atomic radius. Similar results were also observed by other worker [4,7,10]. Because, after low heat treatment these implanted species diffuse out from silicon crystals and results the silicon island. Figs. 2–5 show successive AFM images of a Si (1 0 0) surface of the domain boundary with carbon, nitrogen, oxygen and argon ion after irradiation. Si islands are formed selectively along the domain boundary after ion irradiation. Although the small silicon islands soon disappear, larger ones survive. Silicon islands beyond the critical size do not disappear after low temperature annealing. New Si islands are also observed along domain boundaries. These islands consist of Si bilayer and grow epitaxially on the Si substrate. Silicon islands observed in the AFM images as a function of atomic mass of the implanting species. As ions species atomic mass increases, the shape of the islands becomes blurred and the estimation of the area becomes more difficult.

It is widely known that interstitials and vacancies are introduced in bulk crystals by ion irradiation and that they diffuse during annealing. As for the mechanism of formation of Si islands, there are two possibilities [4,8,9]. One is the immediate out diffusion of the surviving Si interstitials through the subsequent surface migration to domain boundaries. The other is lateral diffusion of Si interstitials beneath to the subsequent out-diffusion of Si through domain boundaries. We believe that the former is more probable for the following reasons. It is known that interstitial Si atoms induced in bulk by ion irradiation diffuse very fast. These interstitial Si atoms reach the surface in a very short time because the depth of these interstitial Si atoms is shallow. This result shows that Si islands are formed along a domain boundary on Si(1 0 0) regardless of the source of the Si atoms supplied during annealing. It may be also possible that sputtered Si atoms return to the surface and contribute to the formation of Si islands.

Fig. 6 shows the AFM results of surface roughness as a function of different implanting species. As the atomic mass of implanting species increases the surface roughness also increases which indicates the variation in size and shape of silicon island, due to the diffusion of vacancies towards the surface with annealing [3,10,11]. Raman spectroscopy is one of the established and precise methods of semiconductor characterization regarding determination of the crystalline structure, disorder and amorphization. It is very sensitive to ion implantation induced defects and any irregularity in the crystalline symmetry.

Fig. 7 shows the Raman spectra for the irradiated silicon with carbon, nitrogen, oxygen and argon implanted ions. The sharp and high intensity peak seen in the spectra at around 522 cm^{-1} for the

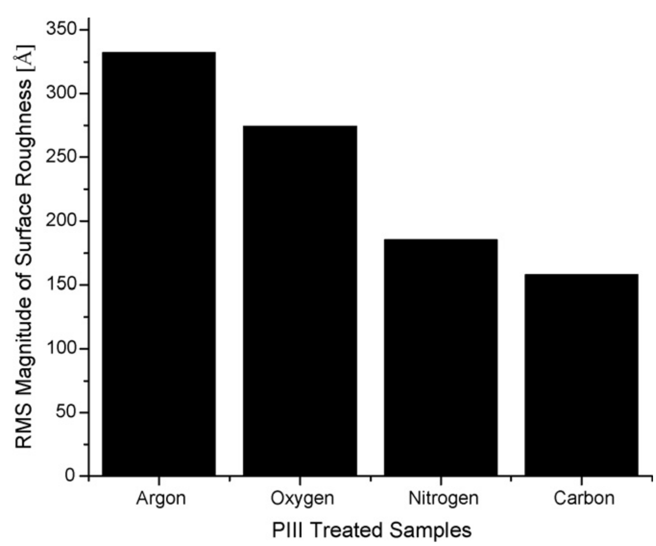

Fig. 6. Surface roughness [RMS (Å)] of PIII treated silicon wafers.

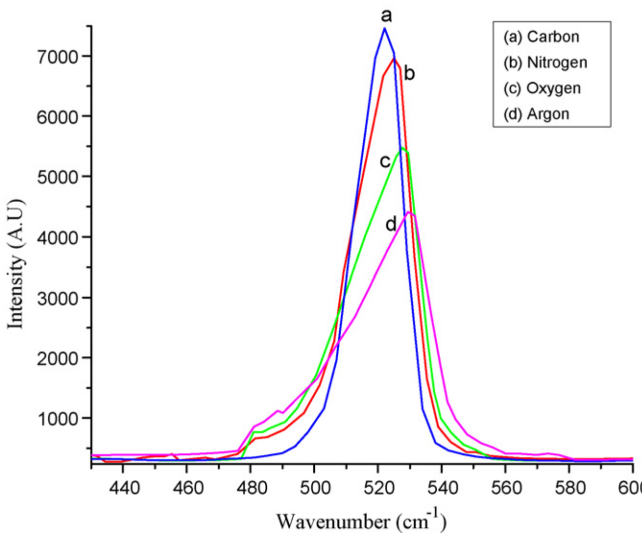

Fig. 7. Raman spectra of the carbon, nitrogen, oxygen and argon PIII, treated silicon substrates.

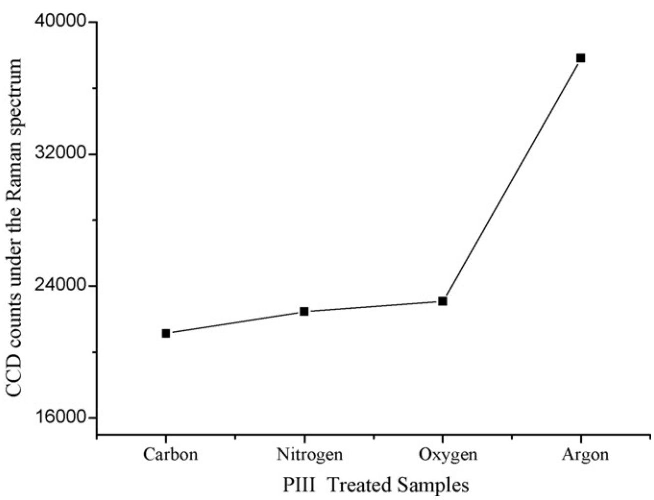

Fig. 8. Area under the Raman spectra of the PIII treated samples.

carbon irradiated specimen corresponds to the transverse optic (TO) phonon of silicon [12,13]. As a result of the nitrogen, oxygen and argon ions irradiation, the red shift was observed from wavenumbers 524, 527 and 530 cm^{-1}, respectively. This behaviour attributed to increasing the Si–Si bonds breaking and increasing the disorder in the silicon matrix. This leads to a reduction in the intensity and broadening of the width of peak with the nitrogen, oxygen and argon irradiated silicon samples. It was observed that irradiation shift the peak intensity towards the lower side of frequency [12,15]. This indicates that disordered in the crystalline silicon matrix depends upon the size of implanted ions even at the same energy and dose of implanting species. Fig. 8 shows the area under the irradiated samples, which is used as the quantitative identification of the level of damage in the implanted region [14,15]. The area under the Raman peak attributes to the defects generation on silicon surface. A systematically increase in the area under the peak and full width half maxima (FWHM) of the resultant dominating peaks were also observed, which indicated that the amorphosation of the silicon increases with increasing the mass of implanting ions, due to increasing the defects in the silicon surface as shown in Fig. 9. These results support our previous AFM observation of PIII treated silicon surfaces.

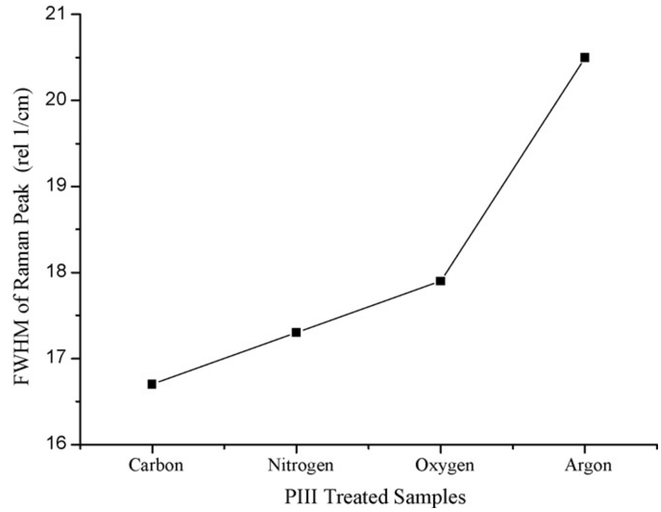

Fig. 9. FWHM of the Raman spectra of the PIII treated samples.

5. Conclusion

The effects on surface topography and morphology of carbon, nitrogen, oxygen and argon plasma immersion ion implantation treated silicon surfaces were investigated using AFM and Raman techniques. The AFM results showed that PIII treatment increased the surface roughness of silicon wafers and formed the silicon island. The Raman study showed, a significant decrease in the intensity of the dominating Raman peaks and increase in the FWHM of the peaks with increasing implantation species mass.

Acknowledgment

The authors would like to acknowledge the help of Dr. Ashutosh Sharma, Prof. and coordinator of DST Unit on Nanosciences, Indian Institute of Technology (IIT)-Kanpur, India for providing sample characterization facility in Nanoscience lab. One of the authors (SKS) acknowledges the useful discussions held with Prof. Dinesh Kumar, Dr B. Prasad, Dr. Raj Kumar and P. J. George, Electronic Science Department, Kurukshetra University, India.

References

[1] I.F. Husein, C. Chan, S. Qin, P.K. Chu, Journal of Physics D: Applied Physics 33 (2000) 2869–2874 (printed in the UK).
[2] W. Möller, S. Mukherjee, Current Science 83 (3) (2002) 237.
[3] A. Piatkowska, G. Gawlik, J. Jagielski, Applied Surface Science 141 (1999) 333–338.
[4] R. Karmouch, Y. Anahory, J.-F. Mercure, D. Bouilly, M. Chicoine, G. Bentoumi, R. Leonelli, Y.Q. Wang, F. Schiettekatte, Physical Review B 75 (2007) 075304.
[5] J.V. Mantese, I.G. Brown, N.C. Cheung, G.A. Collins, MRS Bulletin 21 (1996) 52.
[6] D.T.-K. Kwok, IEEE Transactions on Plasma Science 34 (4) (2006) 1059.
[7] J.B. Mitchell, P.P. Pronko, J. Shewchun, D.A. Thompson, J.A. Davies, Journal of Applied Physics 46 (1) (1975) 332.
[8] J.B. Mitchell, J. Shewchun, D.A. Thompson, J.A. Davies, Journal of Applied Physics 46 (1) (1975) 335.
[9] Y. Glukhoy, M. Rahman, G. Popov, A. Usenko, H.J. Walitzki, Surface & Coatings Technology 196 (2005) 172–179.
[10] T. Seki, T. Aoki, J. Matsuo, I. Yamada, Nuclear Instruments and Methods in Physics Research B 164 (2000) 650.
[11] M. Sadiq, S. Ahmad, M. Shafiq, M. Zakaullah, Nuclear Instruments and Methods in Physics Research B 252 (2006) 219–224.
[12] J. Macıa, E. Martın, A. Pérez-Rodríguez, J. Jiménez, J.R. Morante, B. Aspar, J. Margail, Journal of Applied Physics 82 (8) (1997) 15.
[13] T. Motooka, Thin Solid Films 272 (1996) 235–243.
[14] H. Bhuyan, M. Favre, E. Valderrama, G. Avaria, F. Guzman, H. Chuaqui, I. Mitchell, E. Wyndham, R. Saavedra, M. Paulraj, Applied Surface Science 254 (2007) 197–200.
[15] J.K.N. Lindner, R. Zuschlag, E.H. te Kaat, Nuclear Instruments and Methods in Physics Research North-Holland B 62 (1992) 314–318.